

ORIGINAL ARTICLE

Simulation of conversion profiles inside a thick dental material photopolymerized in the presence of nanofillers

Samir Bayou¹, Mohamed Mouzali¹, Faten Aloui², Laurence Lecamp² and Philippe Lebaudy²

In dental composites, the presence of inorganic fillers in the organic matrix leads to a light-scattering phenomenon that modifies the light intensity and, consequently, the ultimate polymerization yield. In this study, we aimed to characterize the impact of light scattering on the photopolymerization profiles inside thick materials. First, the photopolymerization kinetics of dental composites containing alumina or zirconia nanofillers were studied. An optimal formulation based on 75 wt% Bis-GMA, 25 wt% triethyleneglycoldimethacrylate and 1 wt% camphorquinone/dimethylaminoethylmethacrylate (1/1) was determined. The compatibility between the organic matrix and the fillers was enhanced by grafting a silane coupling agent onto the surfaces of the nanoparticles. This grafting improved the mechanical properties of the final composites without modifying the photopolymerization kinetics. The presence of nanofillers leads to a light-scattering phenomenon that influences the photoinitiated polymerization yield inside the composite. Thus, to characterize this phenomenon, a four-flux radiative transfer theory was applied to calculate the decrease in the light intensity crossing the dental composite. The conversion profiles were then calculated and compared with experimental ones.

Polymer Journal (2013) 45, 863–870; doi:10.1038/pj.2012.226; published online 9 January 2013

Keywords: dental material; light scattering; nanocomposite; nanofiller; photopolymerization

INTRODUCTION

Dental composites for restoration in odontology are made of an organic matrix that is strengthened by fillers of various natures (mineral or organic). The organic matrix consists of two monomer types: a high molecular weight monomer, assuring the rigidity of the material, and a low molecular weight monomer, making the material more fluid. The most common monomer used for the organic phase in dental restoration materials is the so-called Bis-GMA. The aromatic ring of the material confers rigidity and resistance upon the resin. However, the high viscosity of Bis-GMA is incompatible with clinical use in dentistry and does not permit a high amount of fillers, even though an increase in filler content tends to improve the mechanical properties and to reduce the volume shrinkage and thermal expansion coefficient. Thus, triethyleneglycoldimethacrylate (TEGDMA) is normally added to Bis-GMA. This low-viscosity monomer favors cross-linking by increasing resin conversion. However, this monomer induces high-volume shrinkage during polymerization. Many investigations have been performed to identify new dimethacrylate monomers that do not have these disadvantages,¹ but at the moment, the results are not significant enough to envisage a change in the monomer composition.^{2,3} Because of its outstanding performance, camphorquinone (CQ) with

N,N-dimethylaminoethylmethacrylate (DMAEMA) has been recognized as an extremely valuable photoinitiating system for light curing dental resin composites.⁴ Additionally, inorganic fillers, such as ZrO₂ and Al₂O₃, are commonly used as a radiopacifying agent and to enhance the mechanical properties, respectively.^{5,6}

Monomers, the photoinitiating system and fillers constitute a set of parameters that influence the photopolymerization kinetics, volume shrinkage and mechanical properties of the composite material.^{7–15} Additionally, composite properties are well known to be influenced by the resin–filler interface. Thus, for example, the grafting of low-polar groups onto silanol functions on silica particle surface limits the formation of hydrogen bonds, which lead to aggregation, allowing a better dispersion of the filler in the polymer matrix.^{16,17} Moreover, good adhesion at the resin–filler interface is necessary to limit phase segregation. To promote matrix–filler adhesion, the grafting of coupling agents having photopolymerizable groups on their surfaces was developed.^{18,19}

Today, the emergence of nanotechnology offers new perspectives on the dental material field. In fact, the nanometer scale allows the multiplication of the polymer–filler interface area by 10. Therefore, higher filler amounts can be incorporated into the organic matrix without a major increase in its viscosity, leading to nanocomposites

¹Laboratoire d'Etudes Physico-Chimiques des Matériaux, Application à l'Environnement (LEPCMAE), USTHB, Faculté de Chimie, Bab Ezzouar, Algérie and ²Normandie Université, INSA de Rouen, CNRS UMR 6270, FR 3038, Avenue de l'Université, Saint Etienne du Rouvray, France
Correspondence: Dr L Lecamp, Normandie Université, INSA de Rouen, CNRS UMR 6270, FR 3038, Avenue de l'Université, BP 08, 76801 Saint Etienne du Rouvray, France.
E-mail: laurence.lecamp@insa-rouen.fr

Received 6 July 2012; revised 6 November 2012; accepted 6 November 2012; published online 9 January 2013

that exhibit lower volume shrinkage and higher mechanical resistance.²⁰ However, the decrease in particle size enhances the light-scattering phenomenon, which is one of the parameters that limit the thickness of the photopolymerizable composite layer. Thick materials can only be obtained under light curing due to a layer-by-layer process. Hence, an investigation of the influence of light scattering on the polymerization yield is necessary to characterize the evolution of the photochemical reaction.

This work is broken up into two parts. The first part presents experimental results about the kinetic behavior of a classical dental formulation, loaded or not with alumina or zirconia nanofillers. The effect of the composition of the formulation (reactive diluent/monomer ratio) and of light intensity on conversion was particularly investigated. The knowledge of polymerization kinetics is indispensable to, first, supply significant information about the parameters that can modify monomer conversion and to, second, obtain products with optimal properties. The influence of nanofiller functionalization on the photochemical reaction kinetics and on the mechanical properties of the nanocomposites was also studied.

In the second part of this paper, the previous results were used to numerically simulate conversion profiles inside dental composites. The simulation of these conversion profiles requires knowledge of the light intensity evolution inside the material. So, the light intensity variation was calculated using a four-flux theory.^{21,22} This theory, based on radiative transfer models, is useful for describing light scattering in this type of material²³ and requires the measurement of the specular and diffuse reflectances and of the direct and diffuse transmittances of the dental composites. Validation of the obtained results was performed by comparing them with experimental ones. The conversion profiles inside the material were then calculated as a function of the type and amount of nanofillers. This study was conducted using 465 nm monochromatic light radiation, which is usually used in dental restoration.

Such a study has never been performed on dental materials until now and will permit the determination of the maximal thickness that can be photopolymerized as a function of filler amount and type.

EXPERIMENTAL PROCEDURE

Materials

2,2-bis[4-(2-hydroxy-3-methacryloyloxyprop-1-oxy)phenyl]propane (Bis-GMA, 98%) and TEGDMA (95%, containing 200 p.p.m. of monomethylether hydroquinone) were used as a monomer and reactive diluent, respectively. 3-(methacryloxy)propyl trimethoxysilane (3-MPTS, 98%) was used as a coupling agent. The photoinitiating system was a mixture of CQ (>98%) and 2-(dimethylamino)ethyl methacrylate (DMAEMA, 99%), used in a 1/1 (w/w) ratio. All of these components were purchased from Aldrich (Lyon, France) and used as received without further purification.

The filler Aerosil OX50 (Evonik, Frankfurt am Main, Germany) was zirconia with an average specific surface area (BET) of 50 m²g⁻¹ and an average particle diameter less than 100 nm. The filler Al₂O₃ C (Evonik) was alumina with an average specific surface area (BET) of 100 m²g⁻¹ and an average particle diameter of 10 nm.

Silanization of the filler nanoparticles

A volume of 0.2 ml of 3-MPTS was dissolved in 100 ml of water, and the pH was adjusted by adding acetic acid until the pH reached 4. After 15 min in an ultrasonic bath, 1 g of ZrO₂ was added to the solution. The mixture was then stirred in the ultrasonic bath for 2 h. Finally, a condensation reaction was performed by placing the mixture in a 120 °C oven for 4 h.

The same protocol was used to functionalize the Al₂O₃ filler. The amounts used were 1 ml of 3-MPTS and 2 g of Al₂O₃, and the condensation reaction was performed for 7 h.

After the condensation reaction, the functionalized nanofillers were washed three times with water, three times with chloroform, then filtrated and dried at 120 °C for 2 h.

The nanoparticle grafting yield was determined by thermogravimetric analysis (TGA Q500, TA Instruments, New Castle, DE, USA). Grafted particles were first heated for 1 h at 100 °C to remove any water that was adsorbed on the filler surface. A 6 °C min⁻¹ heating rate was then applied up to 800 °C. The amount *Q* (μmol m⁻²) of grafted 3-MPTS was calculated as follows:²⁴

$$Q = \frac{W_i - W_f}{S_{\text{spec}} \times M \times W_i} \times 10^6$$

where *W_i* and *W_f* (g) are the sample weight at 100 °C and 800 °C, respectively; *M* (g mol⁻¹) is the molecular weight of the grafted fragment; and *S_{spec}* (m² g⁻¹) is the specific area of the filler particles.

Preparation and characterization of the photocurable (un)loaded mixtures

For unloaded photocurable mixtures, Bis-GMA and TEGDMA were first heated for 30 min at ~50 °C. Then, 1 wt% of the photoinitiating system CQ/DMAEMA (1/1) (w/w) was added under stirring in the dark at a concentration ranging 0.5–1.25 wt% relative to the reaction mixture.

For loaded photocurable suspensions, a 75/25 (w/w) Bis-GMA/TEGDMA formulation containing 1 wt% CQ/DMAEMA (1/1 w/w) was homogeneously mixed with the nanofillers (DAC 150 FVZ-K Speed Mixer, Flack Teck, Landrum, SC, USA) for 5–15 min at 3500 r.p.m. The filler concentration ranged from 20–50 wt% for Al₂O₃ and from 50–80 wt% for ZrO₂.

The viscosities of the (un)loaded formulations were measured using the controlled stress rheometer AR 2000 (TA Instruments) with a Peltier temperature control device. The storage (*G'*) and loss (*G''*) moduli were measured as a function of frequency at the desired temperature (usually 25 °C) under low applied stress (*σ*) in the linear viscoelasticity domain, where no intermolecular ruptures occur. The linearity of the viscoelastic properties was carefully checked for all investigated mixtures before measuring the *G'* and *G''* moduli. Two types of measuring geometries were used: a cone with a diameter of 40 mm and an angle of 2° for the unloaded formulations and a plate geometry for the loaded ones.

Photopolymerization kinetics monitoring

Two techniques were used to monitor the photopolymerization kinetics: differential scanning calorimetry, which allowed a thermal study (not presented in this paper), and real-time infrared spectroscopy.

During differential scanning calorimetry (DSC7 Perkin Elmer, Waltham, MA, USA), heat flow versus time was recorded at 30 °C under a nitrogen atmosphere. The light source is a 500 W halogen lamp (LA500 Blue Light, Philippine Union Commercial Inc., New Manila Quezon City, Philippines), emitting a quasi-monochromatic radiation at 465 nm. The optical part of the calorimeter, sample preparation and treatment of the thermogram were described elsewhere.²⁵ The computation of the conversion and reaction rate was performed according to a previously published work.²⁶

The photopolymerization kinetics were monitored using real-time Fourier transform infrared spectroscopy (Perkin Elmer FTIR 2000 spectrometer) with an attenuated total reflection accessory (ATR MK II Golden Gate, Specac, Eurolabo, Paris, France). A reaction mixture drop was deposited and spread over the ATR diamond crystal using a glass slide to ensure uniformity of the surface analysis. A quasi-monochromatic radiation at 465 nm, coming from the aforementioned 500 W halogen lamp, was placed in the FTIR spectrometer sample chamber so that it would not interfere with the IR beam. All kinetics measurements were performed at 30 °C. The disappearance of methacrylate double bonds was observed at 1636 cm⁻¹. A reference band at 1715 cm⁻¹, assigned to the carbonyl group, was used to calculate conversions. The

conversion of the methacrylate groups can be calculated by measuring the absorbance at each reaction time and determined as follows:

$$\chi(t) = 100 \times \frac{\frac{A_0^{1636}}{A_0^{715}} - \frac{A_t^{1636}}{A_t^{715}}}{\frac{A_0^{1636}}{A_0^{715}}}$$

where $\chi(t)$ is the conversion of the methacrylate groups at time t , A_0 is the initial absorbance (before UV irradiation) and A_t is the absorbance at time t .

For both techniques, the light intensity (in lux) was measured at the sample surface using a light meter (Amprobe LM-100, Glottetal, Germany), taking into account the energy absorbed by the glass slide. The measured values were then converted into irradiance (mW cm^{-2}).

Optical measurements

The diffuse reflectance and diffuse transmittance were measured at 465 nm using an S2000 Ocean Optics spectrophotometer (I.D.I.L. Fibres Optiques, Lannion, France) equipped with an integrating sphere. The obtained values allowed the determination of the scattering and absorption coefficients, as described in well-known works.^{27,28}

Physicochemical properties of the photocured materials

Samples were analyzed by dynamical mechanical analysis (DMA 7 Perkin Elmer) in compression mode using a stainless steel parallel plate probe (1 mm in diameter) at a 1 Hz frequency and $10^\circ\text{C min}^{-1}$ heating rate. The static and dynamic forces applied were 450 and 350 mN, respectively. The mechanical transition temperature T_α was measured at the maximum of the $\tan \delta$ curve.

The Persoz hardness was determined in seconds using a SP0500 pendulum apparatus (Labomat, Saint Denis, France). Three measurements were taken per sample.

RESULTS AND DISCUSSION

Photopolymerization of unloaded mixtures

The influence of various parameters (the Bis-GMA/TEGDMA ratio and light intensity) was investigated first to obtain the optimal dental resin properties and the parameters necessary for simulation.

Bis-GMA and TEGDMA were mixed in various weight proportions with 1 wt% of the photoinitiating system CQ/DMAEMA (1/1 w/w). Thin films ($40\ \mu\text{m}$) of these mixtures were irradiated with a $100\ \text{mW cm}^{-2}$ light intensity. The evolution of the conversion and reaction rate for different TEGDMA concentrations was determined using differential scanning calorimetry measurements. The viscosities of the mixtures before light exposition and the T_α of the light-cured materials are listed in Table 1. Figure 1a shows that the final conversion increases with increasing TEGDMA concentration. This

result could be explained by a synergistic effect of the mixture components on the polymerization yield, which is most likely due to a reduction in the resin viscosity, as shown in Table 1, and to the plasticizing effect of TEGDMA on Bis-GMA.⁷ This assumption is in agreement with the fact that the initial reaction rate is higher than those for each monomer separately, irrespective of the mixture composition. The reaction rate reaches a maximum at $\sim 37.5\ \text{wt\%}$ TEGDMA (Figure 1b). There is most likely competition between the plasticizing effect and the reactivity of the monomers, and the reactivity is dominant at high TEGDMA concentrations. As can be seen in Figure 1b, the polymerization rate curve of TEGDMA (curve 6) shows a shoulder at $\sim 5\ \text{s}$ of irradiation. This shoulder was mentioned by Cook²⁹ and Dickens *et al.*³⁰ and was attributed to intramolecular cyclization at the beginning of the polymerization.¹⁰ Thus, the propagation initially occurs more extensively via an intramolecular attack on the radical site of the pendant double bond (primary cyclization). This intermolecular attack leads to network formation (crosslinking). Finally, the polymerization yield is never quantified because of the limited mobility of the reactive species when vitrification occurs (Table 1).

The optimal composition (Bis-GMA/TEGDMA 75/25 (w/w)) was studied for different light intensity values (Figure 2). Although these results and related considerations are well known,^{25,31} they are necessary for the simulation study.

Photopolymerization of loaded mixtures

Composites containing non-grafted nanoparticles. The organic matrix having Bis-GMA blended with TEGDMA in a 3/1 ratio was mixed with ZrO_2 ($<100\ \text{nm}$) or Al_2O_3 (10 nm) in various weight

Table 1 Viscosities of the formulations at 20°C and mechanical transition temperatures of the photopolymerized formulations

TEGDMA (wt%)	Al_2O_3 (wt%)	ZrO_2 (wt%)	Viscosity (Pa s)	T_α ($^\circ\text{C}$)
0	0	0	67.0	65.6
12.5	0	0	12.7	73.4
25	0	0	7.5	74.3
37.5	0	0	6.6	81.0
50	0	0	5.6	85.3
100	0	0	4.8	87.0
25	20	0	4016	—
25	30	0	$3.5 \cdot 10^7$	—
25	40	0	n.d. ($>3.5 \times 10^7$)	—
25	0	50	7.6	—
25	0	60	48.1	—
25	0	70	2460	—
25	0	80	n.d. (>2500)	—

Abbreviation: n.d., not determined.

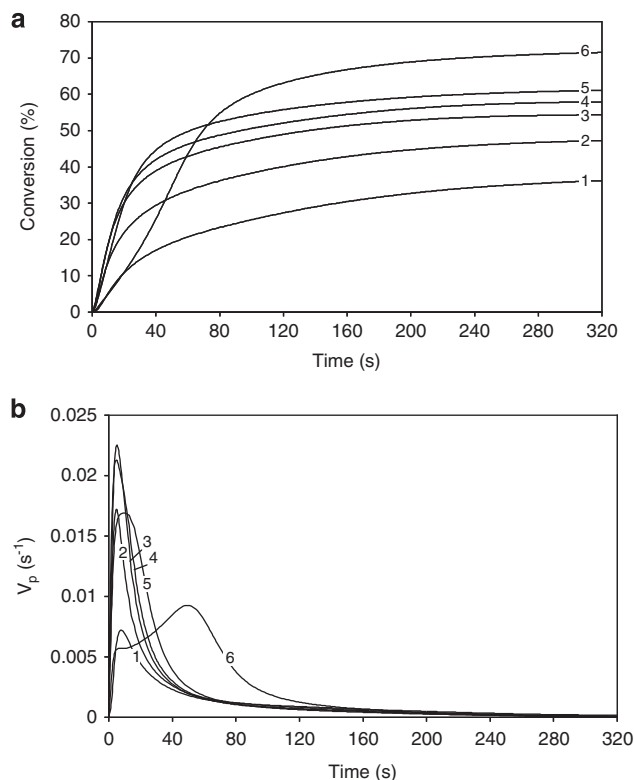


Figure 1 Evolution of the double bond conversion (a) and reaction rate (b) of the organic matrix for different TEGDMA concentrations in the presence of 1 wt% CQ/DMAEMA (1/1). 1: 0 wt%; 2: 12.5 wt%; 3: 25 wt%; 4: 37.5 wt%; 5: 50 wt%; 6: 100 wt%.

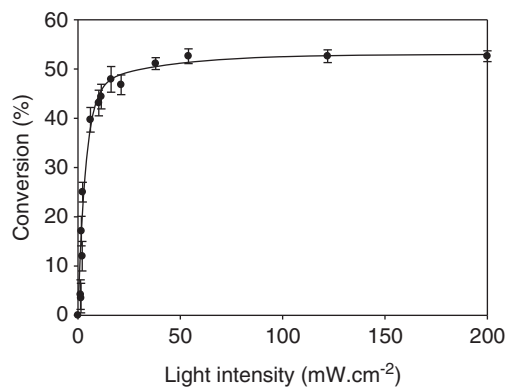


Figure 2 Evolution of the final double bond conversion versus the light intensity for a 75/25 (w/w) Bis-GMA/TEGDMA formulation.

Table 2 Results of the 3-MPTS grafting onto the filler particle surfaces

Filler	Al ₂ O ₃	ZrO ₂
Amount of 3-MPTS used in silanization (wt%)	52.0	20.8
TGA weight loss (%)	12.3	3.1
Grafting yield (%)	36.9	18.5
Amount of grafted 3-MPTS ($\mu\text{mol m}^{-2}$)	6.1	3.0

Abbreviation: 3-MPTS, 3-(methacryloxy)propyl trimethoxysilane.

proportions. The viscosities of the mixtures before light exposure are listed in Table 2. Because of the higher viscosities of the Al₂O₃-based formulations compared with those of the ZrO₂-based ones, photopolymerized films of identical thicknesses could not be realized. So, 0.11-mm-thick films with Al₂O₃ and 0.05-mm-thick films with ZrO₂ were irradiated with a 230 mW cm⁻² light intensity. Hence, no comparison between the fillers was made and only the influence of the filler amount on the kinetics was investigated. The final conversion and reaction rates were determined using FTIR measurements.

Despite the high increase in the photocurable formulation viscosity upon addition of a filler (Table 2), several works have demonstrated that the conversion is not affected by the global viscosity of the loaded suspension; it only depends on the viscosity of the intergranular phase.^{32,33} As the viscosity of the intergranular phase is constant, the small decrease in the final polymerization yield observed for the conversion curves plotted in Figure 3 can only be related to a decrease in the light intensity within the material. In fact, the presence of fillers in a photocurable formulation leads to a light-scattering phenomenon that can be influenced by the number, size and refractive index of the particles.^{33–35} The consequence of this scattering is a higher decrease in the light intensity inside the material than the one induced by the absorption of the reaction medium. Hence, irrespective of the filler, the deterioration in the ultimate conversion versus the filler amount indicates a decrease in the light intensity on the analyzed surface, which is related to an increase in the number of scattering centers.

Composites containing grafted nanoparticles. The grafting of a coupling agent onto the particle surface to enhance the compatibility of the mineral microfillers with the organic matrix has been described in many works.^{18,36,37} 3-MPTS is a classic and efficient silane coupling agent that is usually used to functionalize silica particles. Moreover,

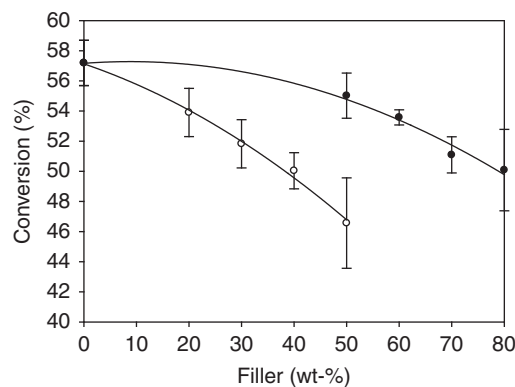


Figure 3 Evolution of the final double bond conversion of a 75/25 (w/w) Bis-GMA/TEGDMA formulation versus the nanofiller concentration: (o) Al₂O₃; (●) ZrO₂.

Table 3 Persoz hardness of dental materials containing Al₂O₃ or ZrO₂ nanofillers

	Persoz hardness (s) of formulations containing	
	non-grafted nanofillers	3-MPTS-grafted nanofillers
Unloaded resin	235 ± 3	
20 wt% Al ₂ O ₃	213 ± 2	219 ± 1
50 wt% Al ₂ O ₃	206 ± 6	247 ± 1
50 wt% ZrO ₂	197 ± 3	251 ± 3
80 wt% ZrO ₂	191 ± 3	288 ± 1

owing to the covalent bonds that can be formed under light exposure, its methacrylate group enables good compatibilization of the fillers.

In this study, alumina and zirconia particles were also grafted with 3-MPTS. The grafting yield and amount of 3-MPTS grafted onto the filler particles were quantitatively determined by thermogravimetric analysis. The results are presented in Table 2. TGA of the samples shows a one-step weight loss that occurred between 200 and 600 °C, indicating that all of the silane molecules were chemically bonded to the surfaces of the fillers because physically adsorbed silane molecules would be removed at lower temperatures (50–150 °C).

Various amounts of functionalized fillers were introduced into the 75/25 (w/w) Bis-GMA/TEGDMA formulation. The kinetics of these new suspensions were monitored using FTIR and compared with that obtained for the same conditions with non-functionalized fillers. The results show that the functionalization of the fillers does not greatly influence the kinetic curves. The ultimate polymerization yield slightly decreases in the presence of grafted particles, but this decrease is attenuated when the filler amount increases. However, a compatibilization effect was clearly observed in the mechanical properties of the nanocomposites. In fact, irrespective of the filler, the addition of non-functionalized nanoparticles led to a decrease in the Persoz hardness, as observed in other works,³⁸ whereas an increase in the Persoz hardness was observed in the presence of grafted fillers (Table 3).

As the chemical modification of the nanoparticle surfaces did not greatly affect the phenomena that govern the photopolymerization kinetics, the following study was performed using nanocomposites with non-grafted particles.

Photopolymerization of thick dental nanocomposites

Experimental measurement of the polymerization and light intensity gradients. The direct measurement of the conversion and light

intensity inside a thick material during a photochemical reaction is not possible. Nevertheless, when the photopolymerization kinetics are monitored by a FTIR apparatus fitted with an ATR accessory, the analyzed sample surface corresponds to one that is not directly exposed to the light beam. Hence, the use of samples with different thicknesses enables the determination of these parameters in an indirect way.

Figure 4 shows the conversion kinetics of a 75/25 (w/w) Bis-GMA/TEGDMA formulation containing either 20 wt% of alumina or 50 wt% of a zirconia powder for different polymerized thicknesses. As expected, the thicker the sample, the lower the conversion for a given reaction time. The ultimate experimental conversion will be compared with the calculated one later (Figure 8).

Using the conversion curves previously obtained for thin layers as a function of light intensity (Figure 2), the ultimate experimental conversion measured for the sample bottom can easily be converted into the light intensity value received by this side of the sample (Figure 5). The light intensity decrease is due to the influence of both the light absorption and scattering on the conversion. These results must be compared with the calculated ones presented in Figure 7.

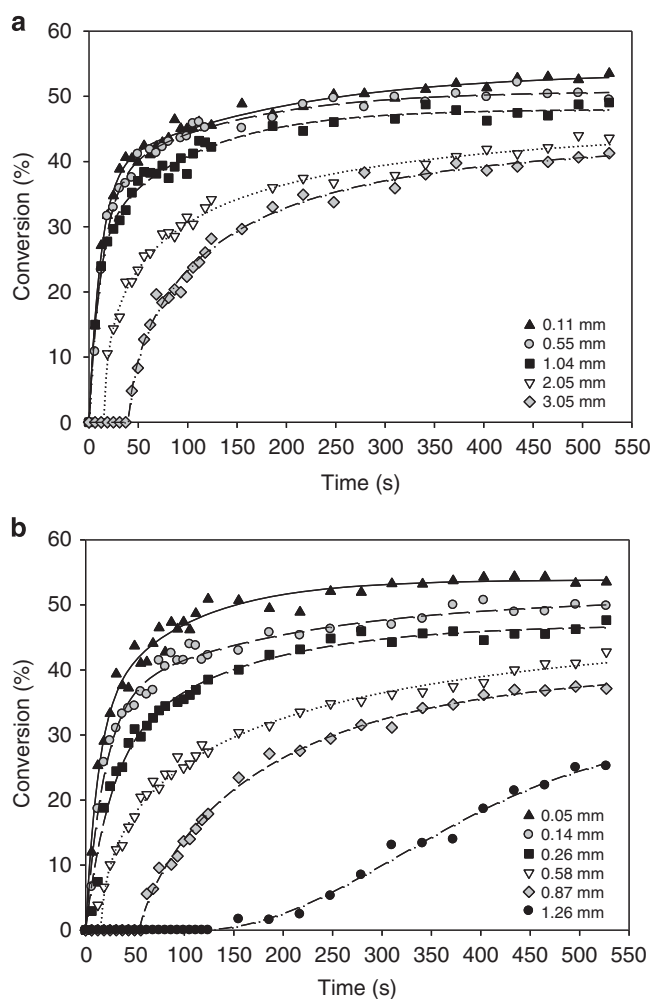


Figure 4 Evolution of the final double bond conversion of a 75/25 (w/w) Bis-GMA/TEGDMA formulation versus the thickness under an incident light intensity $I_0 = 230 \text{ mW cm}^{-2}$ for: (a) 20 wt% Al_2O_3 ; (b) 50 wt% ZrO_2 .

Calculation of the light intensity and polymerization gradients. In a scattering medium, the use of the Beer–Lambert law to describe radiative flux behavior is no longer justified because the path of the light beam through the material is not rectilinear. Therefore, a four-flux model was used to calculate the radiative flux. In this model, the irradiation is assumed to be perpendicular to the sample surface, and the radiation field consists of four contributions: two collimated intensities (I_λ^+ , the direct transmittance, and I_λ^- , the specular reflectance) and two diffuse radiation intensities (L_λ^+ , the diffuse transmittance, and L_λ^- , the diffuse reflectance), as indicated in Scheme 1. In the following study, λ is equal to 465 nm.

The scattering and absorption of light by the medium result in a decrease in the intensities of the collimated beams (I_λ^+ and I_λ^-). The intensity of the diffuse beam L_λ^+ decreases not only due to absorption but also due to scattering into the backward hemisphere (relative to the direction of the incident radiation); the intensity increases due to the scattering of I_λ^+ , I_λ^- and L_λ^- into the forward hemisphere. The same behavior is observed for the other diffuse beam L_λ^- . Consequently, the differential equations for the four intensities are

$$\frac{\partial I_\lambda^-}{\partial x} - K_\lambda I_\lambda^- - \sigma_{\lambda r} I_\lambda^- - \sigma_{\lambda t} I_\lambda^- = 0 \quad (1)$$

$$\frac{\partial I_\lambda^+}{\partial x} - K_\lambda I_\lambda^+ - \sigma_{\lambda r} I_\lambda^+ - \sigma_{\lambda t} I_\lambda^+ = 0 \quad (2)$$

$$\frac{\partial L_\lambda^-}{\partial x} - 2(K_\lambda + \sigma_{\lambda r})L_\lambda^- + 2\sigma_{\lambda r}L_\lambda^+ = -(\sigma_{\lambda r}I_\lambda^+ + \sigma_{\lambda t}I_\lambda^-)/\pi \quad (3)$$

$$\frac{\partial L_\lambda^+}{\partial x} - 2(K_\lambda + \sigma_{\lambda r})L_\lambda^+ + 2\sigma_{\lambda r}L_\lambda^- = -(\sigma_{\lambda r}I_\lambda^- + \sigma_{\lambda t}I_\lambda^+)/\pi \quad (4)$$

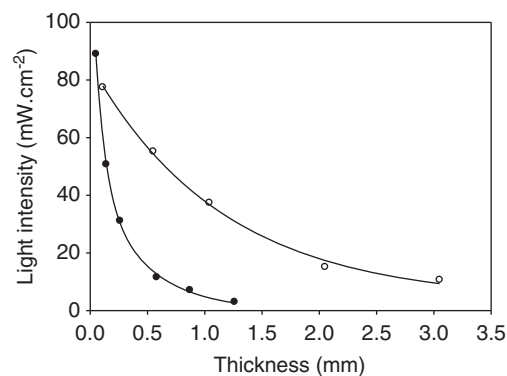
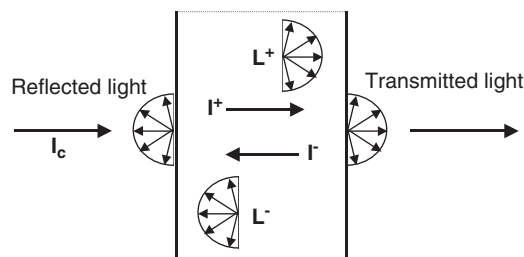


Figure 5 Evolution of the light intensity received by the photopolymerizable formulation versus the crossed thickness for: (o) 20 wt% Al_2O_3 ; (•) 50 wt% ZrO_2 .



Scheme 1 Schematic representation of the four contributions to the radiation field inside an inhomogeneous sample that is normally illuminated.

where x is the position along the depth of the sample, $\sigma_{\lambda t}$ is the transmittance scattering coefficient, $\sigma_{\lambda r}$ is the reflectance scattering coefficient and K_λ is the absorption coefficient.

The solution for this system has been described in another work:³⁴

$$I_\lambda^- = I_{m\lambda} \exp(\beta_\lambda x) \quad (5)$$

$$I_\lambda^+ = I_{p\lambda} \exp(-\beta_\lambda x) \quad (6)$$

$$L_\lambda^- = a_\lambda^- \exp(-\gamma_\lambda x) + b_\lambda^- \exp(\gamma_\lambda x) + c_\lambda^- \exp(-\beta_\lambda x) + d_\lambda^- \exp(\beta_\lambda x) \quad (7)$$

$$L_\lambda^+ = a_\lambda^+ \exp(-\gamma_\lambda x) + b_\lambda^+ \exp(\gamma_\lambda x) + c_\lambda^+ \exp(-\beta_\lambda x) + d_\lambda^+ \exp(\beta_\lambda x) \quad (8)$$

Where

$$\gamma_\lambda = 2[K_\lambda(K_\lambda + \sigma_{\lambda t} + \sigma_{\lambda r})]^{1/2} \quad (9)$$

and β_λ is the extinction coefficient:

$$\beta_\lambda = (K_\lambda + \sigma_{\lambda t} + \sigma_{\lambda r}) \quad (10)$$

Generally, for the sake of simplicity, $\sigma_{\lambda r} = \sigma_{\lambda t} = \sigma_\lambda$,³⁹ and Equation (10) can be written as

$$\beta_\lambda = (K_\lambda + 2\sigma_\lambda) \quad (11)$$

The optical properties of the dental material, obtained using the integrating sphere, are listed in Table 4. These properties give the boundaries conditions that make it possible to calculate Equations 5, 6, 7 and 8 and, therefore, make it possible to obtain the light intensity inside the sample. For the 1.55-mm-thick composite containing 80 wt% ZrO₂, light was absorbed completely, so it was not possible to obtain these boundaries' conditions and consequently to simulate the conversion profiles. In Table 4, we note that the reflectance values increased with an increase in the Al₂O₃ concentration.

From the spectroscopic results, the evolution of the flux involved in the polymerization reaction rate was calculated for the different formulations, assuming an initial incident radiation intensity of 100 mW cm⁻² at 465 nm. The results are presented in Figure 6. The collimated flux I_λ^+ (Figure 6a) is energetically the main flux. The decrease in this flux inside the sample is due to absorption and scattering. The backward collimated beam I_λ^- (Figure 6b) is energetically weak because it arises from the I_λ^+ reflectance from the interface of the sample substrate. As far as the diffuse beam L_λ^+ evolution is concerned (Figure 6c), the shift in the L_λ^+ maximum versus the Al₂O₃ concentration can be explained by a competition between the decrease in the light intensity and the increase in the number of scattering particles as a function of the sample thickness. In Figure 6d, the backward scattering beam (L_λ^-) behavior can be explained using the same argument.

Figure 7 shows the evolution of ϕ_λ for formulations containing 20 wt% and 50 wt% Al₂O₃ and 50 wt% ZrO₂. These simulated fluxes ϕ_λ result from the addition of the four previous fluxes and are consistent with the experimental ones presented in Figure 5. As expected, the higher the Al₂O₃ concentration, the higher the decrease in ϕ_λ versus thickness.

Knowing the light behavior at 465 nm and the conversion kinetic parameters, the simulation of the conversion gradient profile in a dental material is now possible. The simulation was performed using

Table 4 Spectral reflectances and transmittances for different thicknesses and Al₂O₃ or ZrO₂ concentrations

Filler	Thickness (mm)	Transmittance (%)	Reflectance (%)
Al ₂ O ₃ (20 wt%)	1.75	8	20
Al ₂ O ₃ (50 wt%)	1.45	2.5	35
ZrO ₂ (50 wt%)	1.60	1	35
ZrO ₂ (80 wt%)	1.55	0	80

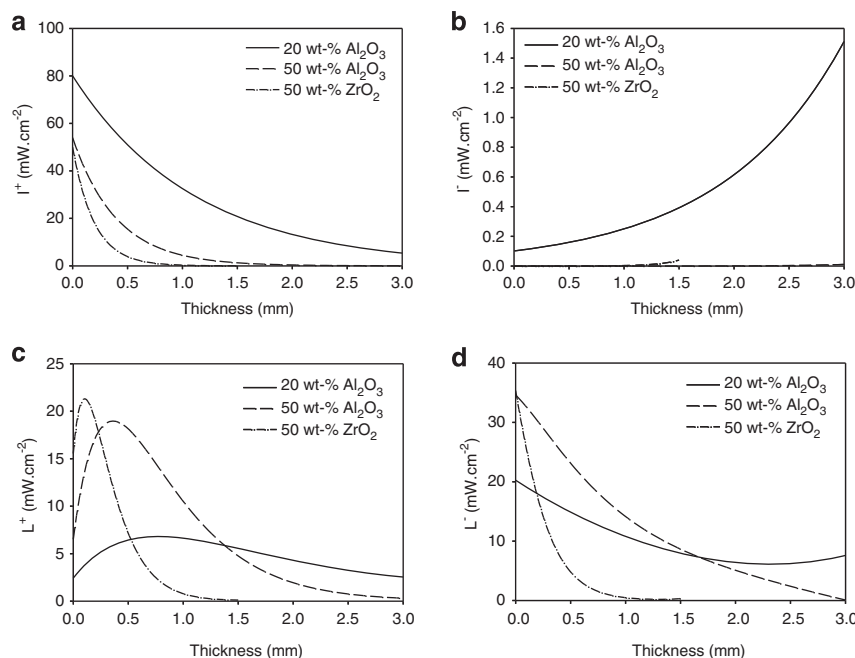


Figure 6 Simulation of the evolution of the four fluxes versus the sample thickness for different fillers at various concentrations: (a) I^+ ; (b) I^- ; (c) L^+ ; (d) L^- .

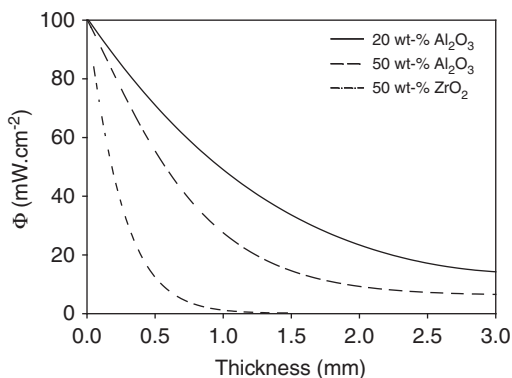


Figure 7 Evolution of the total flux versus the sample thickness for different fillers at various concentrations.

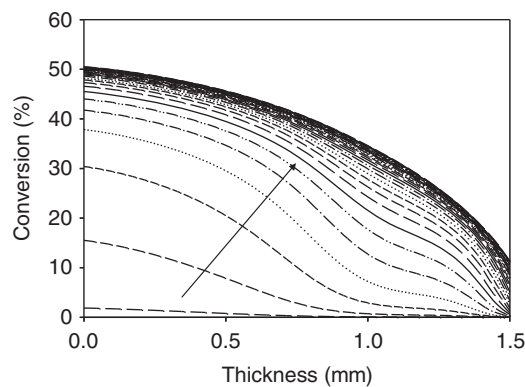


Figure 9 Simulation of the conversion evolution versus the thickness for a 50 wt% ZrO₂-based composite.

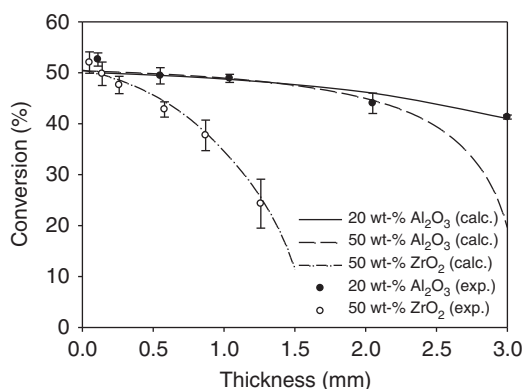


Figure 8 Calculated (lines) and experimental (dots) ultimate conversion versus the thickness for different fillers at various concentrations.

a multiphysics modeling package (Femlab, Comsol, Paris, France). All of the simulations were calculated using an incident irradiation of 100 mW cm⁻² at 465 nm. Several assumptions were made:

- (i) The temperature is constant.
- (ii) The conversion kinetic parameters are only functions of the irradiation light intensity.
- (iii) The optical parameters are constant during the process.

The conversion C versus the thickness x can phenomenologically be described according to the following differential equation:⁴⁰

$$\frac{dC_x}{dt} = k(\phi_\lambda(x)) \cdot [f(\phi_\lambda(x)) - C_x]^2 \cdot C_x^{0.8} \quad (12)$$

where k and f are functions calculated from experimental values.

Full details about this numerical procedure are given in a previous work.⁴¹

Figure 8 shows the final experimental and calculated conversions versus the sample thickness. Taking the experimental errors into account, the calculated values are in good agreement with the experimental ones. As expected, the higher the decrease in ϕ_λ versus depth, the lower the conversion. For a concentration of 50 wt% Al₂O₃, it appears that the conversion was very weak when the thickness was larger than 3 mm. This photopolymerizable thickness was reduced to 1.5 mm for a 50 wt% ZrO₂-based formulation.

Figure 9 shows the conversion evolution versus the sample thickness every 20 s for a composite containing 50 wt% ZrO₂. This

simulation clearly shows that it is not possible to reduce the polymerization gradient by increasing the photopolymerization time.

CONCLUSIONS

The photopolymerization kinetics of a dental formulation based on Bis-GMA and TEGDMA in optimal concentrations were determined in the presence and absence of alumina or zirconia nanofillers. A compatibilization of the nanofillers in the organic matrix was implemented by grafting a silane coupling agent onto the nanoparticles. The grafting did not impact the photopolymerization kinetics. However, as expected, the mechanical properties of the nanocomposites were enhanced.

A four-flux radiative transfer theory was applied to predict the light behavior inside thick scattering and absorbing dental nanocomposites. Conversion profiles in the nanocomposite material were obtained by numerical modeling. This simulation enabled the determination of the maximum thickness that can be polymerized. Thus, for a composite containing 50 wt% ZrO₂ nanoparticles, the thickness cannot exceed 0.5 mm without strongly affecting the polymerization yield, which affects the properties of the composite. For a composite containing 20 wt% Al₂O₃ nanoparticles, up to a 3-mm-thick sample can be polymerized without considerable variation in the polymerization yield. From the obtained results, it can be observed that the photopolymerizable thickness depends on the amount and type of the fillers.

- 1 Buruiana, T., Melinte, V., Stroea, L. & Buruiana, E. C. Urethane dimethacrylates with carboxylic groups as potential dental monomers. synthesis and properties. *Polym. J.* **41**, 978–987 (2009).
- 2 Sankarapandian, M., Shobba, H. K., Kalachandra, S., Mc Grath, J. E. & Taylor, D. F. Characterization of some aromatic dimethacrylates for dental composite applications. *J. Mater. Sci. Mater. Med.* **8**, 465–468 (1997).
- 3 Labella, R., Braden, M., Clarke, R. L. & Davy, K. W. M. THFMA in dental monomer systems. *Biomaterials* **17**, 431–436 (1996).
- 4 Dart, E. C. & Nemcek, J. Photopolymerizable composition. GB Patent 1408265 (1971).
- 5 Amirouche, A., Mouzali, M. & Watts, D. C. Radiopacity evaluation of BisGMA/TEGDMA/opaque mineral filler dental composites. *J. Appl. Polym. Sci.* **104**, 1632–1639 (2007).
- 6 Abboud, M., Vol, S., Duguet, E. & Fontanille, M. PMMA-based composite materials with reactive ceramic fillers. Part III: Radiopacifying particle reinforced bone cements. *J. Mater. Sci. Mater. Med.* **11**, 295–300 (2000).
- 7 Sideridou, I., Tserki, V. & Papanastasiou, G. Effect of chemical structure on degree of conversion in light-cured dimethacrylate-based dental resins. *Biomaterials* **23**, 1819–1829 (2002).

- 8 Viljanen, E. K., Skrifvars, M. & Vallittu, P. K. Dendritic copolymers and particulate filler composites for dental applications: degree of conversion and thermal properties. *Dent. Mater.* **23**, 1420–1427 (2007).
- 9 Schneider, L. F. J., Cavalcante, L. M., Consani, S. & Ferracane, J. L. Effect of co-initiator ratio on the polymer properties of experimental resin composites formulated with camphorquinone and phenylpropanedione. *Dent. Mater.* **25**, 369–375 (2009).
- 10 Sideridou, I. D., Achilias, D. S. & Karava, O. Reactivity of benzoyl peroxide/amine system as an initiator for the free radical polymerisation of dental and orthopaedic dimethacrylate monomers: effect of the amine and monomer chemical structure. *Macromolecules* **39**, 2072–2080 (2006).
- 11 Neumann, M. G., Schmitt, C. C., Correa, I. C. & Goi, B. E. The effect of using mixed initiator system on the efficiency of photopolymerization of dental resins. *J. Braz. Chem. Soc.* **19**, 1413–1417 (2008).
- 12 Teshima, W., Nomura, Y., Tanaka, N., Urabe, H., Okazaki, M. & Nahara, Y. ESR study of camphorquinone/amine photoinitiator systems using blue light emitting diodes. *Biomaterials* **24**, 2097–2103 (2003).
- 13 Xu, H., Wu, G. & Nie, J. Synthesis and photopolymerization characteristics of amine coinitiator. *J. Photochem. Photobiol. A* **193**, 254–259 (2008).
- 14 Ellakwa, A., Cho, N. & Lee, I. B. The effect of resin matrix composition on the polymerization shrinkage and rheological properties of experimental dental composites. *Dent. Mater.* **23**, 1229–1235 (2007).
- 15 Lee, J. H., Um, C. M. & Lee, I. B. Rheological properties of resin composites according to variations in monomer and filler composition. *Dent. Mater.* **22**, 515–526 (2006).
- 16 Ou, Y. C., Yu, Z. Z. & Vidal, A. Effects of alkylation of silicas on interfacial interaction and molecular motions between silicas and rubbers. *J. Appl. Polym. Sci.* **59**, 1321–1328 (1996).
- 17 Karabela, M. M. & Sideridou, I. D. Effect of the structure of silane coupling agent on sorption characterisation of solvents by dental resin-nanocomposites. *Dent. Mater.* **24**, 1631–1639 (2008).
- 18 Antonucci, J. M. & Dickens, S. H. Chemistry of silanes: interfaces in dental polymers and composites. *J. Res. Natl. Inst. Stand. Technol.* **110**, 541–558 (2005).
- 19 Bauer, F., Sauerland, V. & Glasel, H. J. Preparation of scratch and abrasion resistant onto nanoparticles. 3. Effect of filler particles and grafting agents. *Macromol. Mater. Eng.* **287**, 546–552 (2002).
- 20 Beun, S., Glorieux, T., Devaux, J. & Vreven, J. Characterization of nanofilled compared to universal and microfilled composites. *Dent. Mater.* **23**, 51–59 (2007).
- 21 Maheu, B., Letoulouzan, J. N. & Gouesbet, G. Four-flux models to solve the scattering transfer equation in terms of Mie parameters. *Appl. Opt.* **23**, 3353–3362 (1984).
- 22 Dangoux, R., Bissieux, C. & Egee, M. *Thermal transfer in composite materials* (Eurotherm 4, Nancy, 1988).
- 23 Vargas, W. Optical properties of pigmented coatings taking into account particle interactions. *J. Quant. Spectrosc. Rad.* **78**, 187–195 (2003).
- 24 Bourgeat-Lami, E., Herrera, N. N., Putaux, J. L., Reculosa, S., Perro, A., Ravaine, S., Mingotaud, C. & Duguet, E. Surface assisted nucleation and growth of polymer latexes on organically-modified inorganic particles. *Macromol. Symp.* **229**, 32–46 (2005).
- 25 Lecamp, L., Youssef, B., Bunel, C. & Lebaudy, P. Photoinitiated polymerization of a dimethacrylate oligomer: 1 Influence of photoinitiator concentration, temperature and light intensity. *Polymer* **38**, 6089–6096 (1997).
- 26 Sideridou, I. D., Achilias, D. S. & Kostidou, N. C. Copolymerization of dental dimethacrylates initiated by a benzoyl peroxide/amine redox system. *J. Appl. Polym. Sci.* **109**, 515–524 (2008).
- 27 Kortüm, G. *Reflectance spectroscopy: Principles, methods, applications* (Springer Verlag, New York, 1969).
- 28 Taira, M. & Yarnaki, M. Studies on optical properties of a visible-light-cured dental composite resin by diffuse reflectance measurements. *J. Mater. Sci. Lett.* **14**, 198–200 (1995).
- 29 Cook, W. D. Photopolymerization kinetics of oligo(ethylene oxide) and oligo(methylene) oxide dimethacrylates. *J. Polym. Sci. Polym. Chem.* **31**, 1053–1067 (1993).
- 30 Dickens, S. H., Stansbury, J. W., Choi, K. M. & Floyd, C. J. E. Photopolymerization kinetics of methacrylate dental resins. *Macromolecules* **36**, 6043–6053 (2003).
- 31 Dvidenko, N., Garcia, O. & Sastre, R. Photopolymerization kinetics of dimethacrylate-based Light-cured dental resins. *J. Appl. Polym. Sci.* **97**, 1016–1023 (2005).
- 32 Atai, M. & Watts, D. C. A new kinetic model for the photopolymerization shrinkage-strain of dental composites and resins. *Dent. Mater.* **22**, 785–791 (2006).
- 33 Badev, A., Abouliatim, Y., Chartier, T., Lecamp, L., Lebaudy, P., Chaput, C. & Delage, C. Photopolymerization kinetics of a polyether acrylate in the presence of ceramic fillers used in stereolithography. *J. Photochem. Photobiol. A* **222**, 117–122 (2011).
- 34 Azan, V., Lecamp, L., Lebaudy, P. & Bunel, C. Simulation of the photopolymerization gradient inside a pigmented coating. Influence of TiO₂ concentration on the gradient. *Prog. Org. Coat.* **58**, 70–75 (2007).
- 35 Griffith, L. & Halloran, J. W. Scattering of ultraviolet radiation in turbid suspensions. *J. Appl. Phys.* **81**, 2538–2546 (1997).
- 36 Sideridou, I. D. & Karabela, M. M. Effect of amount of 3-methacryloxypropyl-trimethoxysilane coupling agent on physical properties of dental resin nano-composites. *Dent. Mater.* **25**, 1315–1324 (2009).
- 37 Wilson, K. S. & Antonucci, J. M. Interphase structure-property relationships in thermoset dimethacrylate nanocomposites. *Dent. Mater.* **22**, 995–1001 (2006).
- 38 Rachini, A. *Nanocomposites argiles-photopolymères: préparation, caractérisation et applications*. Thesis, the Université de Haute-Alsace (2007).
- 39 Désilles, N., Gautrelet, C., Lecamp, L., Lebaudy, P. & Bunel, C. Effect of UV light scattering during photopolymerization on UV spectroscopy measurements. *Eur. Polym. J.* **41**, 1296–1303 (2005).
- 40 Chandra, R. & Soni, K. Studies on kinetics of bulk polymerization of divinyl ester by radical-initiated thermal and photo-polymerization. *Polym. Int.* **31**, 239–245 (1993).
- 41 Lecamp, L., Lebaudy, P., Youssef, B. & Bunel, C. Simulation of conversion profiles and temperature distributions within dimethacrylate thick material during photopolymerization. *Macromol. Symp.* **148**, 77–86 (1999).